Volume 27
Number 2
January 27, 1988

Inorganic Chemistry

Articles

Contribution from the Department of Hydrocarbon Chemistry, Faculty of Engineering, Kyoto University, Kyoto 606, Japan

An Ethylene Glycol Derivative of Boehmite

Masashi Inoue,* Yasuhiko Kondo, and Tomoyuki Inui

Received July 9, 1987

The reaction of gibbsite with ethylene glycol yielded a product having an empirical formula of $AlO(OCH_2CH_2OH)_{0.31}(OH)_{0.69}$. The product had a unique honeycomb-like texture and a high surface area. The XRD pattern and IR spectrum suggest that the product has a layer structure of boehmite with the ethylene glycol moiety incorporated between the boehmite layers through covalent bonding. On calcination, the ethylene glycol moiety decomposed into carbonyl compound(s) and then carbonaceous material but the boehmite structure was well maintained up to 400 °C. Basal spacing of boehmite gradually decreased with the increase in the calcination temperature, suggesting that the carbonyl compound(s) and the carbonaceous material remain between the boehmite layers. Further increase in the calcination temperature resulted in the formation of an X-ray-amorphous transition alumina.

Introduction

The organic derivatives of layered inorganics belong to an interesting class of intercalation compounds in which guest organic moieties are bound through covalent bonding to the layered structure of the host inorganics.[1] However, only a few compounds of this class have been prepared so far. The first example was a methanol derivative of lepidocrocite (FeOOH) reported by Kikkawa et al.,[2] who prepared this compound by substituting the Cl ion of FeOCl with methoxide. They also reported an ethylene glycol derivative of lepidocrocite.[3] Yamanaka reported the formation of an ethylene glycol derivative of zirconium phosphate by a reaction of zirconium phosphate with ethylene oxide.[4,5] His group also have developed a more general method for the preparation of organic derivatives of zirconium phosphate in which the phosphorus acid group is substituted by alkyl phosphate or alkylphosphonate.[6] All these reactions mentioned above are topochemical ones in which the lamellar structures of the original compounds are maintained in the products. On the contrary, Alberti et al. reported direct synthesis of organic derivatives of zirconium phosphate by precipitation from alkyl phosphate or alkylphosphinic acid with Zr(IV).[7] This procedure was extended by Dines and DiGiacomo for synthesis of organic derivatives of a variety of metal(IV) phosphates.[8] The compounds prepared by these direct precipitation methods may not be called intercalation compounds anymore because the starting materials do not have layered structures.

During the course of our long-term study on controlling the pore texture of alumina for a use as a catalyst support,[9] we have found that the thermal treatment of crystalline aluminum hydroxide in an ethylene glycol medium yields a novel derivative of boehmite in which the ethylene glycol moiety is incorporated into the boehmite layers.[10] In this paper, the nature of the bonding between the organic moiety and inorganic layers will be discussed and a novel intercalation compound in which carbonaceous material is incorporated between the layers of boehmite will be reported.

Experimental Section

Reaction of Gibbsite with Ethylene Glycol. A gibbsite sample of fine particle size was prepared by dry grinding of the commercial gibbsite sample (B303, Nippon Light Metal: Na_2O, 0.21%; SiO_2, 0.008%; Fe_2O_3, 0.007%; 20–35 μm) for 1 week on an automortar of alumina (diameter 16 cm). The ground gibbsite had a surface area of 20 m^2/g, and the maximum particle size observed by SEM was less than 0.2 μm.

The gibbsite (30 g) was suspended in 130 mL of ethylene glycol (Wako, guaranteed grade), and the mixture was poured into a test tube of Pyrex glass that was then placed in a 300-mL autoclave. In the gap between the autoclave and the test tube was placed an additional 30 mL of ethylene glycol. The atmosphere in the space of the autoclave was replaced with nitrogen, and then the mixture was heated to 250 °C at a rate of 2 °C/min and held at that temperature for 2 h. After cooling, the resulting precipitates were washed with methanol repeatedly and air-dried.

The product was a white mixture of powders and hard bricks having a bulk density of 0.66 g/cm^3 and a specific gravity of 2.42 g/cm^3 (pycnometer–H_2O). It did not show any observable swelling properties.

(1) Alberti, G.; Costantino, U. In *Intercalation Chemistry*; Whittingham, M. S., Jacobson, A. J., Eds.; Academic: New York, 1982; p 174. Halbert, T. R. *Ibid.*, p 399.
(2) Kikkawa, S.; Kanamaru, F.; Koizumi, M. *Inorg. Chem.* **1976**, *15*, 2195; **1980**, *19*, 262.
(3) Kikkawa, S.; Kanamaru, F.; Koizumi, M. *Inorg. Chem.* **1980**, *19*, 259.
(4) Yamanaka, S. *Inorg. Chem.* **1976**, *15*, 2811. Yamanaka, S.; Tsujimoto, M.; Tanaka, M. *J. Inorg. Nucl. Chem.* **1979**, *41*, 605.
(5) See also: Ortiz-Avila, C. Y.; Clearfield, A. *Inorg. Chem.* **1985**, *24*, 1773.
(6) Yamanaka, S.; Hattori, M. *Chem. Lett.* **1979**, 1073. Yamanaka, S.; Maeda, H.; Tanaka, M. *J. Inorg. Nucl. Chem.* **1979**, *41*, 1187. Yamanaka, S.; Hattori, M. *Inorg. Chem.* **1981**, *20*, 1929. Yamanaka, S.; Sakamoto, K.; Hattori, M. *J. Phys. Chem.* **1984**, *88*, 2067.
(7) Alberti, G.; Costantino, U.; Allulli, S.; Tomassini, N. *J. Inorg. Nucl. Chem.* **1978**, *40*, 1113.
(8) Dines, M. B.; DiGiacomo, P. M. *Inorg. Chem.* **1981**, *20*, 92. Dines, M. B.; Griffith, P. C. *Inorg. Chem.* **1983**, *22*, 567.
(9) Inui, T.; Miyake, T.; Takegami, Y. *J. Jpn. Petrol. Inst.* **1982**, *25*, 242. Inui, T.; Miyake, T.; Fukuda, K.; Takegami, Y. *Appl. Catal.* **1983**, *6*, 165.
(10) Inoue, M.; Kondo, Y.; Inui, T. *Chem. Lett.* **1986**, 1421.

0020-1669/88/1327-0215$01.50/0

Anal. Calcd for $Al_2O_3 \cdot 0.62HOCH_2CH_2OH \cdot 0.38H_2O$: C, 10.11; H, 3.07; ignition loss, 30.78. Found: C, 10.00; H, 3.07; ignition loss (1000 °C, 2 h), 30.85.

Characterization. Thermal analysis was performed on a Shimadzu DT-30 thermal analyzer: A weighed amount (ca. 30 mg) of the sample was placed in the analyzer, dried in a 40 mL/min gas flow (dried air or nitrogen) until no more weight decrease was detected, and then heated at the rate of 10 °C/min in the same gas flow. X-ray diffraction (XRD) was measured on a Rigaku Geigerflex-2013 diffractometer employing Cu Kα radiation and an Ni filter. Infrared (IR) spectra were obtained on a Shimadzu IR-435 spectrometer with the usual KBr-pellet technique. Surface areas and nitrogen adsorption isotherms were measured on a Micrometric Accusorb 2100E instrument at 77.4 K employing the conventional constant-volume method. Isotherms and surface areas are quoted for 1 g of outgassed solid without correction for the water or organic moiety remaining after outgassing at 120 °C. Surface areas were calculated by applying the usual BET procedure to the adsorption data, taking the average area occupied by a nitrogen molecule as 16.2 Å^2. Elemental analyses were performed at the Laboratory of Organic Elemental Microanalysis, Kyoto University.

Control Experiments. (1) A boehmite sample (56 m^2/g) was prepared by autoclaving a gibbsite sample (B103, Nippon Light Metal; 6–10 μm; 0.21% Na_2O; 2.4 m^2/g) in butanol at 250 °C. The XRD analysis of the product showed it to be composed of 93% well-crystallized boehmite and 7% unreacted gibbsite.[11] To a 1-g portion of this boehmite was added 1 mL of a methanol solution containing 42.7 mg of ethylene glycol, and the resulting slurry was dried at room temperature with continuous stirring until the sample became a well-divided powder.

(2) To a 1-g portion of the ground gibbsite sample was added 1 mL of a methanol solution containing 58.1 mg ethylene glycol, and the mixture was dried as mentioned above.

(3) A well-crystallized boehmite sample was prepared by hydrothermal treatment of a gibbsite (B303; see above). This boehmite (10 g) was ground on the automortar in the presence of ethylene glycol (10 mL) for 36 h. The resulting thick slurry was washed with methanol and dried in air. The thermal analyses of these samples were performed as mentioned above.

Identification of the Thermal Decomposition Products. In a preliminary experiment, a product (1.1412 g) obtained by autoclaving the ground gibbsite at 300 °C was placed in a porcelain boat that was then set in a quartz tube in a tubular furnace. After the replacement of the atmosphere with nitrogen, the sample was heated to 350 °C at a rate of 2 °C/min and held at that temperature for 30 min in a 40 mL/min flow of nitrogen. The effluent gas was introduced into a condenser immersed in liquid nitrogen. The weight of the calcined sample was 0.9287 g, and 0.1869 g of the liquid decomposition product was collected. Gas chromatographic analysis (Porapak N and PEG 6000 columns) indicated that about 98% of the product was water; 0.95% acetaldehyde, 0.6% ethanol, 0.06% acetone, and 0.07% ethyl acetate were also detected together with traces of unidentified products.

Temperature-programmed decomposition profiles were determined as follows. The same product was tableted and pulverized into about 15 mesh, about 1.1 g of which was placed in a quartz tubular reactor of 8-mm internal diameter equipped with an electric furnace. The sample was heated at a rate of 2 °C/min up to 650 °C and held at that temperature for 30 min in a nitrogen (or air) flow of 14.5 (14.1) mL (STP)/min. Effluent gases were repeatedly analyzed by gas chromatography (Active Carbon and Porapak N and QS columns).

Results and Discussion

Structural Aspects. Boehmite is one of the modifications of aluminum oxide hydroxide, AlOOH.[12] This compound occurs in nature in the European bauxites. It can be prepared by aging aluminum hydroxide gel,[13] by thermal dehydration of coarse gibbsite or bayerite (both modifications of aluminum hydroxide),[14] by oxidation of aluminum metal,[15] by rehydration of transition aluminas,[16] and more commonly by hydrothermal treatment of aluminum hydroxides.[17] The structure of boehmite has been studied by means of X-ray diffraction,[18-20] neutron diffraction,[21] vibrational spectra,[22-24] and NMR spectra.[25,26] Reichertz and Yost[18] first estimated the structure of boehmite on the basis of the fact that boehmite is isomorphous with lepidocrocite, the structure of which was determined by Ewing from oscillation and rotation photographs of a naturally occurring single crystal.[27] All the recent works suggest that the space group of the boehmite structure is D_{2h}^{17} with four AlOOH formula units per nonprimitive unit cell (Figure 1).[20,21,24,26] Each aluminum atom is surrounded by a distorted octahedral group of oxygen atoms, and these octahedral groups are joined by sharing edges in such a way that they form zigzagged layers parallel to the 010 plane. These layers are linked together by hydrogen bonds between hydroxyl groups in neighboring layers. Hydrogen atoms lie on Wyckoff 8f sites with 0.5 occupation.[20,21,24,26]

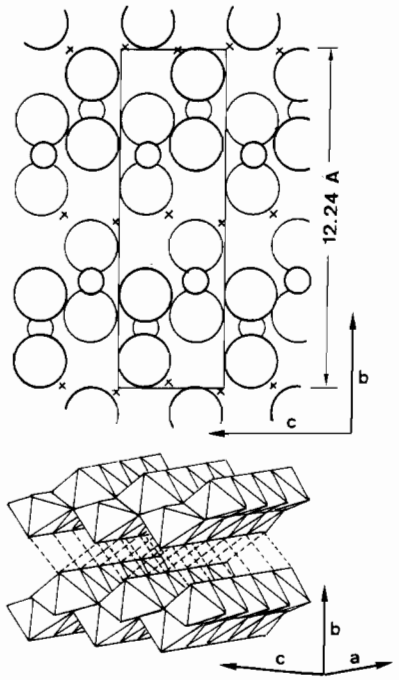

Figure 1. Crystal structure of boehmite.

Although boehmite has a structure closely related to FeOCl, which is a typical host layered compound giving intercalation compounds,[28] intercalation of guest molecules into boehmite layers has never been reported, presumably because of strong hydrogen

(11) Inoue, M.; Kitamura, K.; Tanino, H.; Nakayama, H.; Inui, T. *J. Mater. Sci. Lett.*, in press.
(12) For reviews: Gitzen, W. H. *Alumina as a Ceramic Material*; American Cermic Society, Columbus, OH, 1970. Wefers, K.; Bell, G. M. *Alcoa Tech. Pap.—Alcoa Res. Lab.* **1972**, *No. 19*.
(13) Shimizu, Y.; Miyashige, T.; Funaki, K. *Kogyo Kagaku Zasshi* **1964**, *67*, 788.
(14) Stumpf, H. C.; Russell, A. S.; Newsome, J. W.; Tucker, C. M. *Ind. Eng. Chem.* **1950**, *42*, 1398.
(15) Torkar, K.; Worel, H.; Krischner, H. *Monatsh. Chem.* **1960**, *91*, 653.
(16) Yamaguchi, G.; Chiu, W.-C. *Bull. Chem. Soc. Jpn.* **1968**, *41*, 348.
(17) Ginsberg, H.; Koesler, M. *Z. Anorg. Allg. Chem.* **1952**, *271*, 41. Sato, T. *J. Appl. Chem.* **1960**, *10*, 414.
(18) Reichertz, P. P.; Yost, W. J. *J. Chem. Phys.* **1946**, *14*, 495.
(19) Milligan, W. O.; McAtee, J. L. *J. Phys. Chem.* **1956**, *60*, 273. Farkas, L.; Gadó, P.; Werner, P.-E. *Mater. Res. Bull.* **1977**, *12*, 1213.
(20) Christoph, G. G.; Corbato, C. E.; Hofmann, D. A.; Tettenhorst, R. T. *Clays Clay Miner.* **1979**, *27*, 81. Hill, R. J. *Clays Clay Miner.* **1981**, *29*, 435.
(21) Achiwa, N.; Yamamoto, N.; Kawano, S. *Annu. Rep. Res. React. Inst., Kyoto Univ.* **1977**, *10*, 8. Christensen, A. N.; Lehmann, M. S.; Convert, P. *Acta Chem. Scand., Ser. A* **1982**, *A36*, 303. Corbato, C. E.; Tettenhorst, R. T.; Christoph, G. G. *Clays Clay. Miner.* **1985**, *33*, 71.
(22) Wickersheim, K. A.; Korpi, G. K. *J. Chem. Phys.* **1965**, *42*, 579. Russell, J. D.; Farmer, V. C.; Lewis, D. G. *Spectrochim. Acta, Part A* **1978**, *34A*, 1151. Farmer, V. C. *Spectrochim. Acta, Part A* **1980**, *36A*, 585.
(23) Fripiat, J. J.; Bosmans, H.; Rouxhet, P. G. *J. Phys. Chem.* **1967**, *71*, 1097. Stegmann, M. C.; Vivien, D.; Mazieres, C. *Spectrochim. Acta, Part A* **1973**, *29A*, 1653.
(24) Kiss, A. B.; Keresztury, G.; Farkas, L. *Spectrochim. Acta, Part A* **1980**, *36A*, 653. Kiss, A. B.; Gadó, P.; Keresztury, G. *Spectrochim. Acta, Part A* **1982**, *38A*, 1231.
(25) Holm, C. H.; Adams, C. R.; Ibers, J. A. *J. Phys. Chem.* **1958**, *62*, 992. Kroon, D. J.; Stolpe, C. v. d. *Nature (London)* **1959**, *183*, 944.
(26) Slade, R. C. T.; Halstead, T. K. *J. Solid State Chem.* **1980**, *32*, 119.
(27) Ewing, F. J. *J. Chem. Phys.* **1935**, *3*, 420.
(28) For review: Halbert, T. R. In *Intercalation Chemistry*; Whittingham, M. S., Jacobson, A. J., Eds.; Academic: New York, 1982; Chapter 12.

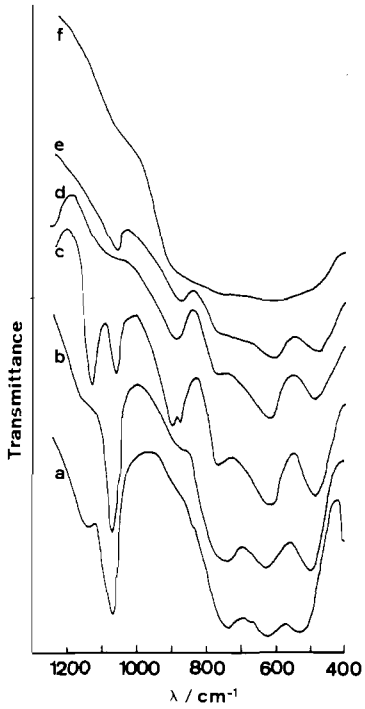

Figure 2. IR spectra: (a) well-crystallized boehmite obtained by hydrothermal treatment of gibbsite; (b) pseudoboehmite obtained by neutralization of $KAlO_2$ with CO_2; (c) the product, $AlO(OCH_2CH_2OH)_{0.31}(OH)_{0.69}$, obtained by the reaction of gibbsite with ethylene glycol at 250 °C for 2 h; (d–f) samples obtained by the calcination of the product at 284, 391 and 500 °C, respectively.

bonding between the layers. A compound known as pseudoboehmite (sometimes also called gelatinous boehmite or boehmite gel) may be regarded as an intercalation compound of boehmite because the extra water molecules in pseudoboehmite are believed to be bound with the hydrogen bridges between the layers of boehmite.[29-31] This compound, however, cannot be synthesized through a reaction of boehmite with water, but rather is usually prepared by aging amorphous alumina gel.[32] Besides water, an organic moiety can also be incorporated between the boehmite layers. Only two examples have been reported thus far. One is "pseudoboehmite-c", reported by Bye and Robinson.[33] They prepared this compound through the hydrolysis of aluminum *sec*-butoxide in 98% ethanol–water and concluded that "some ethanol or alkoxide groups" were incorporated into the boehmite layers.[33] The second example is a compound having an approximate formula of $AlO(OH)_{0.5}(OCH_3)_{0.5}$.[34,35] This compound was prepared by autoclaving gibbsite in methanol at high pressures. Kubo and Uchida concluded that methoxide groups were located between the boehmite layers.[35]

General Features of the Reaction. As briefly reported in the preliminary communication,[10] the reaction of gibbsite with ethylene glycol proceeds autocatalytically with a rather long induction period. Reaction temperatures (200–300 °C) had practically no effect on the product selectivity, and the predominant factor controlling the product selectivity was the particle size of gibbsite. When coarse gibbsite was used, the product was contaminated with well-crystallized boehmite and unreacted gibbsite. Pure product was obtained by using a gibbsite sample of particle size less than 0.2 μm. As we will focus on the chemical and physical properties of the product, the term "the product" hereafter refers to this pure product obtained by the reaction of the gibbsite of fine particle size with ethylene glycol at 250 °C for 2 h, unless otherwise mentioned.

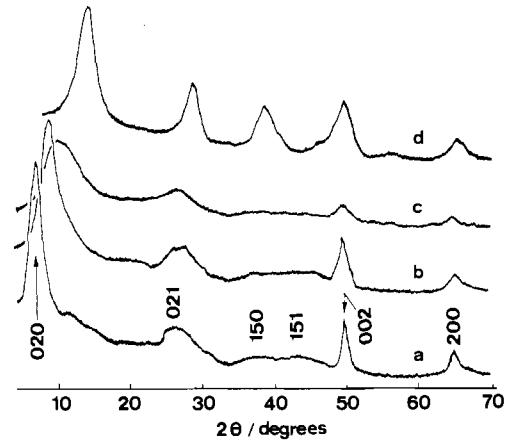

Figure 3. XRD patterns: (a) the product, $AlO(OCH_2CH_2OH)_{0.31}(OH)_{0.69}$; (b, c) samples obtained by calcination of the product at 284 and 391 °C, respectively; (d) pseudoboehmite.

Infrared Spectra. The IR spectrum of the product is shown in Figure 2. Bands characteristic of the boehmite structure were seen at 773, 615, and 478 cm^{-1},[36] suggesting that the product had the layer structure of boehmite. Bands due to the incorporated organic moiety were seen at 3440 s, 2940 m, 2880 m, 1460 w, 1500 m, 1250 w, 1128 m, 1062 m, 900 m, 868 m cm^{-1}, indicating that ethylene glycol moiety was certainly incorporated into the product.

It must be noted that the product showed two absorption bands in the 850–900-cm^{-1} region. This result is in sharp contrast to the result for $FeO(OCH_2CH_2O)_{0.5}$ reported by Kikkawa et al., which showed only one absorption band in this region.[3] As this point, it is important to understand the nature of the bonding between the boehmite layer and the ethylene glycol moiety; we will briefly discuss the vibration modes of ethylene glycol in this region.

Early investigators assigned two IR bands at 865 and 885 cm^{-1} to the rocking vibrations of CH_2 groups.[37] However, using normal-coordinate analysis, Matsuura and Miyazawa assigned the 855-cm^{-1} band to the rocking vibration and the 865-cm^{-1} band to the C–C stretching vibration of the gauche isomer coupled with the C–O stretching mode.[38] Two other groups reached similar conclusions independently.[39]

Miyake prepared two different types of ethylene glycol (monodentate and bidentate) complexes of cobalt and nickel salts and found that the 865-cm^{-1} band shifted to ca. 25 cm^{-1} higher frequency on going from a monodentate to a bidentate complex.[40] Similar shifts were reported for many other complexes.[41,42] This spectral change cannot be attributed to the conformational change

(29) Calvet, E.; Biovinet, P.; Noel, M.; Thibon, H.; Mailard, A.; Tertian, R. *Bull. Soc. Chim. Fr.* **1953**, 99.
(30) Lippens, B. C. Thesis, Delft University of Technology, 1961. Lippens, B. C.; Steggerda, J. J. In *Physical and Chemical Aspects of Adsorbents and Catalysts*; Linsen, B. G., Ed.; Academic: New York, 1970; Chapter 4.
(31) Because of poor crystallinity of pseudoboehmite, the structure of this compound has not yet fully understood. See also: Baker, B. R.; Pearson, R. M. *J. Catal.* **1974**, *33*, 265. Tettenhorst, R.; Hofmann, D. A. *Clays Clay Miner.* **1980**, *28*, 373. Pierre, A. C.; Uhlmann, D. R. *J. Non-Cryst. Solids* **1986**, *82*, 271.
(32) For example: Ginsberg, H.; Huettig, W.; Stiehl, H. *Z. Anorg. Allg. Chem.* **1961**, *309*, 233; **1962**, *318*, 238. Sato, T. *Z. Anorg. Allg. Chem.* **1972**, *391*, 69; *J. Appl. Chem. Biotechnol.* **1974**, *24*, 187.
(33) Bye, G. C.; Robinson, J. G. *Chem. Ind. (London)* **1961**, 1363; *J. Appl. Chem. Biotechnol.* **1974**, *24*, 633.
(34) Bugosh, J. (E. I. du Pont de Nemours & Co.) U.S. Patent 2944916, 1960.
(35) Kubo, T.; Uchida, K. *Kogyo Kagaku Zasshi* **1970**, *73*, 70.
(36) For assignment of these bands, see ref 23 and 24.
(37) Kanbayashi, U.; Nukada, K. *Nippon Kagaku Zasshi* **1963**, *84*, 297. Kuroda, Y.; Kubo, M. *J. Polym. Sci.* **1957**, *26*, 323. Buckley, P.; Giguere, P. A. *Can. J. Chem.* **1967**, *45*, 397.
(38) Matsuura, H.; Miyazawa, T. *Bull. Chem. Soc. Jpn.* **1967**, *40*, 85.
(39) Kirshnan, K.; Krishnan, R. S. *Proc. Indian Acad. Sci.* **1966**, *A64*, 111. Sawodny, W.; Niedenzu, K.; Dawson, J. W. *Spectrochim. Acta, Part A* **1967**, *23A*, 799.
(40) Miyake, A. *Bull. Chem. Soc. Jpn.* **1959**, *32*, 381.
(41) Knetsch, D.; Groeneveld, W. L. *Inorg. Chim. Acta* **1973**, *7*, 81.
(42) Williams, R. M.; Atalla, R. H. *J. Chem. Soc., Perkin Trans. 2* **1975**, 1155.

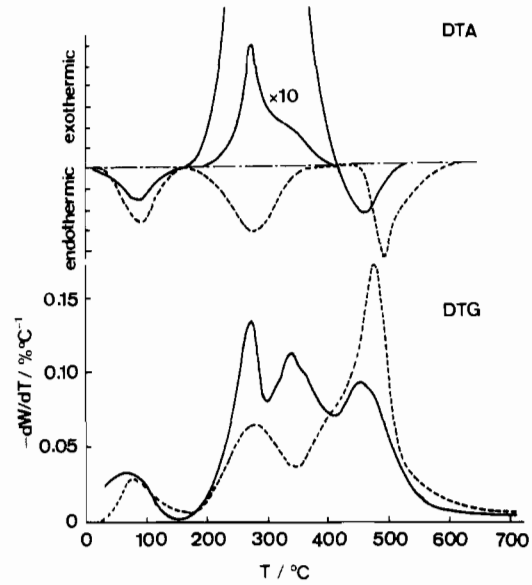

Figure 4. DTG and DTA profiles of the product, $AlO(OCH_2CH_2OH)_{0.31}(OH)_{0.69}$, in an air flow (solid lines) and in a nitrogen flow (broken lines). For the DTA profile in nitrogen flow, thorough replacement of the instrument atmosphere with nitrogen was essential to obtain the endothermic peak at ca. 300 °C. Conditions: 10 °C/min; reference 30 mg of α-alumina; 40 mL/min gas flow.

from a trans conformer to a gauche one because the vibrational spectrum of ethylene glycol in this region is insensitive to the temperature change[43] and because gauche/trans ratios in liquid ethylene glycol determined by Raman spectroscopy[44] and by an NMR technique[45] are in reasonable agreement (gauche/trans = 2–3). As the 865-cm^{-1} band is mainly due to the C–C vibration mode, shifts to higher frequencies may be attributed to the increase in bond order between two carbon atoms. Actually, shortening of the C–C bond in a bidentately coordinated ethylene glycol moiety was reported.[46] As the ethylene glycol moiety in $FeO(OCH_2CH_2O)_{0.5}$ is bidentately bound to a ferric ion, the IR spectrum of this compound can be explained by accidental overlapping of the 885-cm^{-1} band with 865-cm^{-1} band caused by a shift of the 865-cm^{-1} band to higher frequency. The compound reported here showed two bands at 900 and 868 cm^{-1}. These frequencies are quite close to the bands observed in liquid ethylene glycol, which suggests that ethylene glycol moiety is bound monodentately to the boehmite layer and that the remaining hydroxyl end is bound loosely with an adjacent boehmite layer through hydrogen bonding. This argument is also supported by the fact that the hydrogen-bonded OH stretching vibration mode (3440 cm^{-1}) can be seen in the infrared spectrum.

X-ray Diffraction. The X-ray diffraction pattern of the product is given in Figure 3. Proposed assignments for the diffraction peaks are also presented in the figure. An increase in 020 spacing from 6.1 Å for boehmite to 11.6 Å for the product is evident, which indicates clearly that the ethylene glycol moiety is incorporated between layers of boehmite. The XRD pattern is essentially identical with that reported by Bye and Robinson for the product obtained by hydrolysis of aluminum *sec*-butoxide in 98% ethanol–water.[33] However, they did not fully elucidate the structure of their products or the nature of the interaction between boehmite layers and guest moieties.

Thermal Analysis. In an air flow the product decomposed through four successive processes at 80, 270, 339, and 445 °C (Figure 4). The first and the last processes were endothermic, and the remaining two processes were highly exothermic, suggesting oxidative degradation of the ethylene glycol moiety took place at these temperatures. The endothermic nature of the final decomposition suggests that the boehmite structure is broken down at this temperature, which is in good agreement with the temperature for the decomposition of well-crystallized boehmite into a transition alumina.[47] In the nitrogen flow two middle-temperature weight loss peaks shifted toward higher temperatures and the third weight loss peak was merged into the last weight loss peak.

For comparison, three reference samples were prepared and the desorption behavior of ethylene glycol was examined: A well-crystallized boehmite sample having a quite high surface area (56 m^2/g) and the gibbsite sample used as the starting material for the reaction were impregnated with ethylene glycol from methanol solutions and then air-dried. Thermogravimetric traces for these two samples showed that the desorption of ethylene glycol took place around 120 °C in an air flow. Without the gas flow the weight loss peaks shifted slightly toward higher temperature; however, DTA analysis clearly showed that an oxidative reaction did not take place and simple desorption is the origin for the weight loss even without the gas flow. Another well-crystallized boehmite sample was ground in the presence of ethylene glycol for 36 h, followed by washing with methanol and air-drying. For this sample, the TGA trace did not show any weight loss due to the desorption or oxidative degradation of ethylene glycol, suggesting that ethylene glycol was completely washed out with methanol. This must be compared with the procedure for the sample preparation, wherein the sample was repeatedly washed with methanol after the reaction. All these results strongly support the fact that the ethylene glycol moiety is covalently bound to the boehmite layers.

Calcined Products. As TG analyses suggested that the organic moiety decomposed at a lower temperature than the boehmite structure, a new type of layered compound can be expected for the products calcined in the temperature range 270–445 °C; therefore, the nature of the calcined products was examined. The sample was prepared by holding the product at various temperatures for 30 min. The IR spectra and XRD patterns of the thus obtained samples are presented in Figures 2 and 3, respectively. The IR spectra and XRD patterns clearly indicate that the boehmite structure was well maintained up to 400 °C. The boehmite structure was broken down into amorphous alumina at the final decomposition temperature observed by TGA (445 °C). The IR spectrum of the sample calcined at 284 °C showed a band due to the carbonyl groups (1680 cm^{-1}), but bands due to ethylene glycol could not be detected, indicating that ethylene glycol decomposed around 270 °C, leaving carbonyl compound(s) between the boehmite layer. The IR spectrum of the sample calcined at 391 °C showed no characteristic peak due to the organic moiety. As this sample contained 1.9% carbon, the third weight loss can be attributed to the carbonization of carbonyl compound(s), leaving carbonaceous material between the boehmite layers. An interesting feature observed in the XRD patterns is that the 020 spacing decreases with the increase in calcination temperature, which seems to correlate with the successive degradation of the ethylene glycol moiety at temperatures below 445 °C. These results indicate that the product gives other derivatives of boehmite on calcination at medium temperatures.

Decomposition Products. For further insight into the nature of the bonding between the ethylene glycol moiety and the boehmite layers, decomposition products were analyzed. To know the decomposition behavior of ethyelne glycol moiety is also interesting because it can be a model for the catalytic cracking of ethylene glycol.

At low temperatures, formation of acetaldehyde, ethanol, ethyl acetate, and acetone was predominant but ethylene glycol could not be detected. This result suggests that structure **1** is most feasible for the product, where one oxygen atom of the ethylene

(43) Matsuura, H.; Hiraishi, M.; Miyazawa, T. *Spectrochim. Acta, Part A* **1972**, *28A*, 2299.
(44) Schwartz, M. *Spectrochim. Acta, Part A* **1977**, *33A*, 1025.
(45) Connor, T. M.; McLauchlan, K. A. *J. Phys. Chem.* **1965**, *69*, 1888. Pachler, K. G. R.; Wessels, P. L. *J. Mol. Struct.* **1970**, *6*, 471.
(46) Bright, D.; Milburn, G. H. W.; Truter, M. R. *J. Chem. Soc. A* **1971**, 1582. Schroeder, F. A.; Scherle, J.; Hazell, R. G. *Acta Crystallogr., Sect. B: Struct. Crystallogr. Cryst. Chem.* **1975**, *B31*, 531.
(47) Lippens, B. C.; de Boer, J. H. *Acta Crystallogr.* **1964**, *17*, 1312.

Table I. Elemental Analysis[a]

particle size of gibbsite, μm	reacn temp, °C	calcination	% found C	% found H
<0.2[b]	250	as oven-dried[d]	10.00	3.07
		284 °C in air	4.52	3.26
		391 °C in air	1.90	1.80
		700 °C in air	0.51	1.24
<0.2[b]	300	as oven-dried[d]	9.14	3.09
		700 °C in N_2	2.72	1.29
0.2[c]	250	as oven-dried[d]	9.46	3.21
		700 °C in N_2	1.20	0.82

[a] The sample was obtained by the reaction of gibbsite with ethylene glycol at the specified temperature for 2 h followed by calcination. [b] Commercial gibbsite was ground on an automortar for 1 week. See Experimental Section for details. [c] A commercially available sample (B1403, Nippon Light Metal, 11 m^2/g). The product obtained by the reaction of this gibbsite with ethylene glycol contained 1.9% well-crystallized boehmite and 0.3% unreacted gibbsite, as determined by XRD. [d] 130 °C for 2 h.

glycol moiety is incorporated into the boehmite structure and bound to an aluminum ion. On heating, heterolytic cleavage of the C–O bond takes place, leaving the remaining oxygen atom in the boehmite layer. This step may be assisted by the hydroxyl group nearby. The resulting acetaldehyde reacts with another acetaldehyde molecule, yielding ethyl acetate by a Tishchenko type reaction. As the present product has Al–O–C bonds, this reaction proceeds by a mechanism similar to that of the ordinary Tishchenko reaction catalyzed by aluminum ethoxide.[48] Hydrolysis of ethyl acetate yields ethanol and acetic acid. The latter compound further decomposes into acetone. The reaction sequence is summarized in Scheme I.

Above 350 °C, formation of gaseous products, i.e., hydrogen, methane, and lower hydrocarbons, becomes predominant. As all these are reduced products, the carbonaceous material remaining between the boehmite layers must be highly unsaturated. Around 450 °C, formation of water becomes predominant, which corresponds to the collapse of the boehmite layers into a transition alumina. Because carbonaceous material still remains inside the particles, the crystalline structure of the alumina cannot be developed well; therefore, the transition alumina was X-ray amorphous. If the amount of the carbonaceous material remaining after the decomposition can be increased, a new material having a novel structure of alternative layers of graphite and alumina may be formed. Work in this direction is now in progress.

Elemental Analysis. The results for elemental analysis are given in Table I. On the basis of the elemental analysis, the product has an approximate empirical formula of $AlO(OH)_{0.69}(OCH_2CH_2OH)_{0.31}$. One may think that the amount of ethylene glycol incorporated is far less than that expected from the structure; however, because of the following consideration, we concluded that, under the preparation conditions, the space within the boehmite layers is "saturated" with ethylene glycol molecules.

It was assumed that the molecular shape of ethylene glycol is a straight cylindrical lot having a radius of 2.1 Å (estimated from the specific gravity of ethylene glycol at 250 °C and the ordinary van der Waals radius of a methylene group, 2 Å, this enlargement of the methylene radius corresponding to the increase in molecular vibrations) and that these lot-shaped molecules are arranged in the closest packing in a direction perpendicular to the boehmite layers. Then, the maximum number of ethylene glycol molecules for monolayer arrangement within the boehmite layers (see Figure 7) is calculated to be 0.33 per surface oxygen atom. This value is in good agreement with the number of ethylene glycol molecules incorporated into the product (0.31). The above mentioned argument is also supported by the fact that increase in the reaction temperature rather decreased the number of ethylene glycol molecules incorporated into the product.

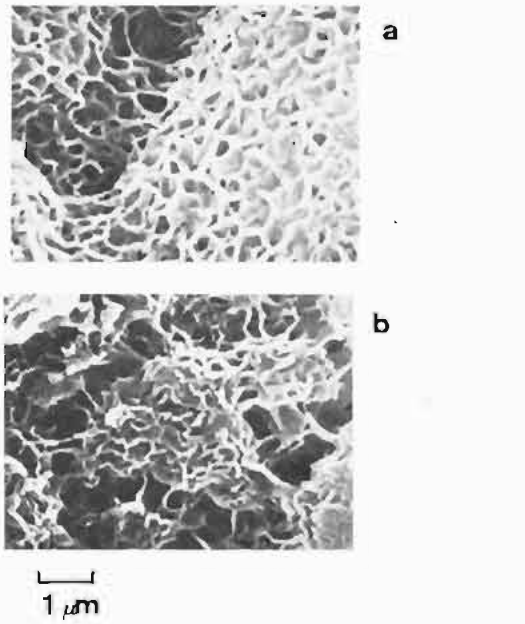

Figure 5. Honeycomb-like texture of the products obtained by the reaction of gibbsite with ethylene glycol: (a) from the ground gibbsite having a particle size less than 0.2 μm; (b) from the commercial gibbsite (see footnote *d* of Table II) having a particle size 70 μm. Note for (b), inside the observable honeycomb-like texture, the unreacted gibbsite core is present.

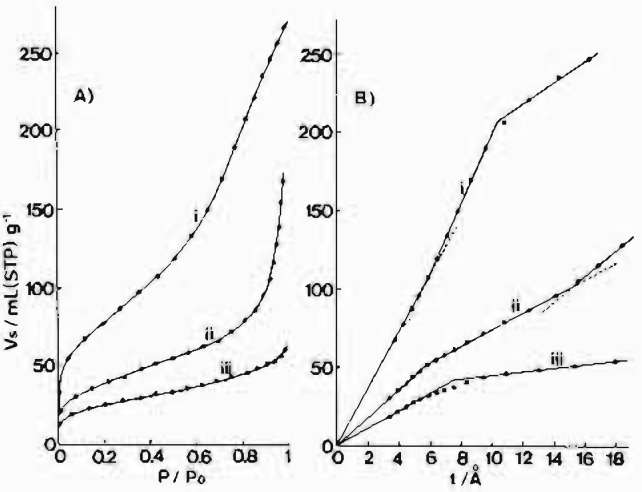

Figure 6. Nitrogen adsorption isotherms of the products obtained by the reaction of gibbsites having the particle sizes of (i) less than 0.2 μm, (ii) 0.2 μm, and (iii) 70 μm with ethylene glycol at 250 °C for 2 h: (A) Ordinary plot; (B) de Boer's *t* plot.

If the lattice parameters, a_0 and c_0, are assumed to be identical with those of well-crystallized boehmite, the specific gravity of the product can be calculated by using the empirical formula and observed basal spacing ($b_0/2$). However, the calculated specific gravity (2.0 g/cm^3) was much smaller than that observed (2.42 g/cm^3). This large discrepancy may be caused by penetration of water molecules between the boehmite layers of the product in measuring the specific gravity.

Morphological Aspects. The most interesting feature of this work is the morphology of the product. As can be seen in Figure 5, the product has a honeycomb-like texture. This result is in sharp contrast to that of the reaction of gibbsite with methanol at high pressure, where a topotactic reaction takes place, yielding a product with hexagonal plate particles.[35] This would indicate that the reaction in ethylene glycol proceeds by completely different mechanisms than the one in methanol at high pressure.

Nitrogen Adsorption Isotherm. The nitrogen adsorption isotherm and de Boer's *t* plot[49] for the product are given in Figure

(48) Lin, I.; Day, A. R. *J. Am. Chem. Soc.* **1952**, *74*, 5133. Ogata, Y.; Kawasaki, A.; Kishi, I. *Tetrahedron* **1967**, *23*, 825. Saegusa, T.; Ueshima, T.; Kitagawa, S. *Bull. Chem. Soc. Jpn.* **1969**, *42*, 248.

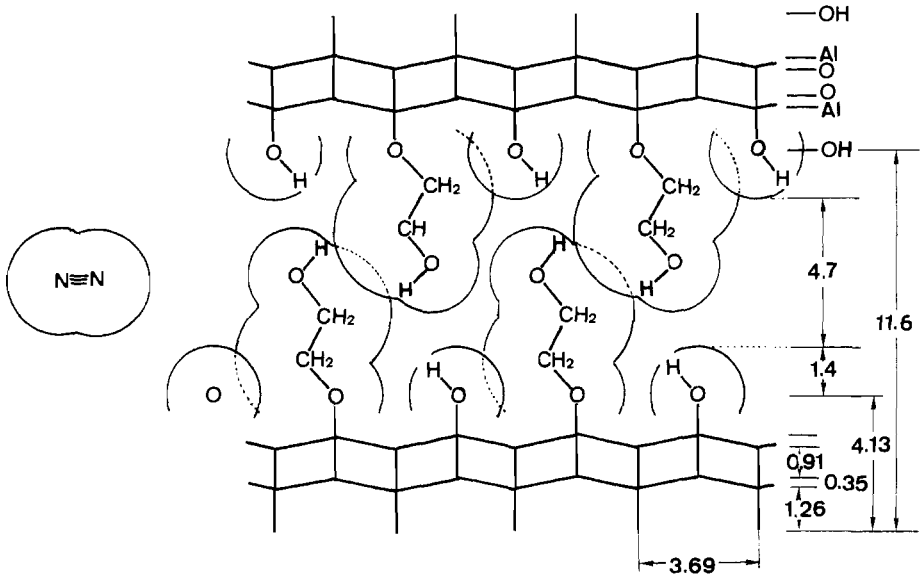

Figure 7. Molecular geometry of $AlO(OCH_2CH_2OH)_{0.31}(OH)_{0.69}$.

Scheme I. Reaction Sequence Yielding the Decomposition Products

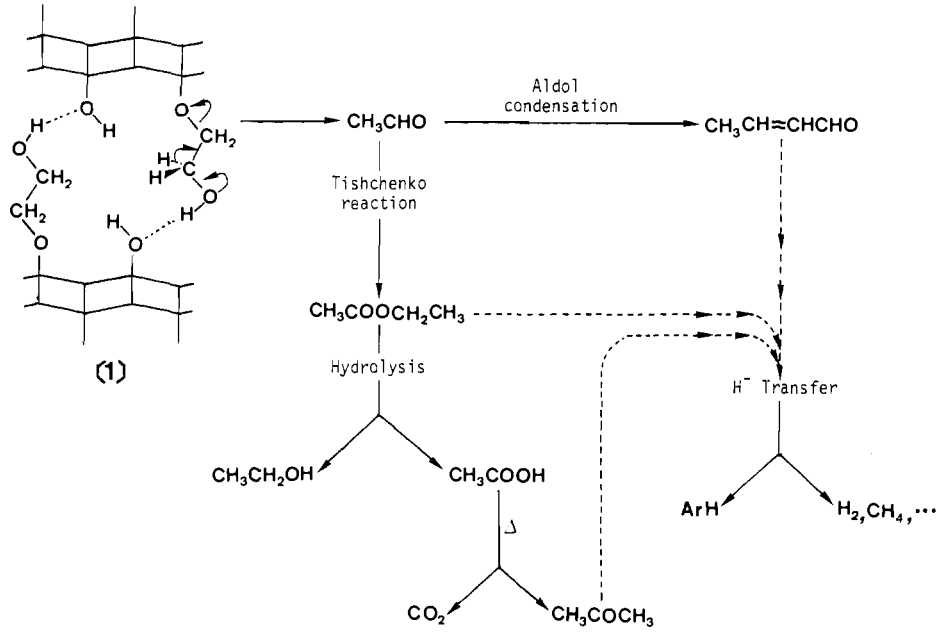

6. For comparison, data for the samples prepared from coarser gibbsites are also plotted in the same figure. The t plots can be divided into three parts. At low relative pressure t plots have large slopes (A region), and from the slopes total surface areas can be calculated. These values are in good agreement with the values calculated by the ordinary BET procedure. When micropores have been filled with adsorbed nitrogen, t plots have small slopes (C region), from which outer surface areas can be calculated. These values are summarized in Table II. If capillary condensation into mesopores takes place, t plots have steeper slopes (B region). For the sample prepared from the coarsest gibbsite, the B region was not observed. For the sample prepared from the gibbsite of 0.2-μm particle size, the B region started at $P/P_0 = 0.9$. For the product obtained from the gibbsite with the finest particle size, mesopores became much narrower and the B region started just after the micropores were filled ($P/P_0 = 0.42$). These mesopores can be explained by wedge-shaped capillaries formed between two sheet crystals of the boehmite derivative, which form a honeycomb-like texture.

(49) Lippens, B. C.; Linsen, B. G.; de Boer, J. H. *J. Catal.* **1964**, *3*, 32. Lippens, B. C.; de Boer, J. H. *J. Catal.* **1965**, *4*, 319.

Table II. Surface Area of the Products of the Reaction of Gibbsite with Ethylene Glycol at 250 °C for 2 h

gibbsite		surface area of the product, m^2/g		
particle size, μm	surface area, m^2/g	S_{BET}[a]	S_T[b]	S_{out}[c]
<0.2	20	279	280	138
0.2[d]	11	138	139	82
70[e]	0.17	88.5	87.7	8.9

[a] Calculated by the ordinary BET procedure. [b] Calculated from the slope of the A region of the de Boer t plot. [c] Calculated from the C region of the de Boer t plot. [d] See footnote c of Table I. [e] A commercially available sample (B73, Nippon Light Metal). The product obtained by the reaction of this gibbsite with ethylene glycol contained 11% well-crystallized boehmite and 41% unreacted gibbsite.

Now, the remaining problem is to determine the origin of the micropores that give the A-region segment in the t plot. Two explanations, (i) spaces between boehmite layers and (ii) defects in stacking the boehmite layers, are possible for the origin of the micropores. The theoretical surface area of boehmite was calculated from the lattice parameters of boehmite to be 1065 m^2/g.

This value is much larger than the observed total surface area. If this value is divided by the total surface area, the number of boehmite layers can be calculated to be 3.8, from which the thickness of the crystallite is calculated to be 44 Å. This value is in good agreement with the crystallite size determined from the Scherrer equation (50 Å). Therefore, we concluded that the micropores come from interstices between crystallites. As the thickness of the platelike crystals, which form the honeycomb-like texture, was 500–2000 Å, defects in stacking the boehmite layers with the openings in micropore range (≤20 Å) are present in the platelike crystals. Moreover, careful examination of the molecular geometry (Figure 7) revealed that gaps between the boehmite layers in the product are too narrow to be accessed by nitrogen molecules, although they may be large enough for water molecules to access the internal surface because hydrogen bondings can be formed. Details of the pore textures of the product and of the aluminas derived from the product will be discussed separately.

Registry No. Water, 7732-18-5; acetaldehyde, 75-07-0; ethanol, 64-17-5; acetone, 67-64-1; ethyl acetate, 141-78-6; nitrogen, 7727-37-9.

Contribution from the Central Research and Development Department,† Experimental Station, E. I. du Pont de Nemours and Company, Wilmington, Delaware 19898, Department of Chemistry, University of New Mexico, Albuquerque, New Mexico 87131, and National Synchrotron Light Source, Brookhaven National Laboratory, Upton, New York 11973

Characterization of Se-Loaded Molecular Sieves A, X, Y, AlPO-5, and Mordenite

John B. Parise,*‡ James E. MacDougall,‡ Norman Herron,‡ Rod Farlee,‡ Arthur W. Sleight,‡ Ying Wang,‡ Thomas Bein,§ Karin Moller,§ and Lee M. Moroney∥

Received January 14, 1987

Selenium has been successfully loaded into molecular sieves A, X, Y, AlPO-5, and mordenite, and the products were characterized by using EXAFS, solid-state NMR, and diffuse-reflectance techniques. This study reveals selenium is predominantly of the trigonal (helical chains) form in all but the A sample, where only the Se_8-crown ring form is found. A mixture of allotropes and helical chains occupy the large 3D-pore and channel systems of molecular sieves X and Y; however, a single, probably fixed-pitch helical-chain allotrope occupies the more constrained 12-membered-ring channels found in mordenite and AlPO-5. The high degree of order in these last two sieves is reflected in a strong second-shell feature in the EXAFS spectra.

Introduction

Because of their restricted pore and channel geometries, molecular sieves are potentially useful for the stabilization of unusual chemical species and finely dispersed bulk materials. Particularly, the effect of semiconductor particle size on electronic, optical, and photocatalytic properties is of great interest. Our interest is in the characterization of semiconductors that are in a size range (10–50 Å) where they neither exhibit semiconductor bulk properties nor show molecular or atomic properties. This "size quantization" effect has been an intense area of study and discussion recently.[1] Molecular sieves, which impose size and geometry constraints on encapsulated materials, yield novel environments for studying this phenomenon.

Classically the characterization of the structure of materials absorbed in molecular sieves has been carried out by using the analysis of the three-dimensional (3D) crystallographic data. However, if the absorbed species is not commensurate with the host lattice, this technique is limited; spectroscopic techniques, sensitive to local structure, prove more useful. In this report, we present results of a study of selenium-loaded molecular sieves (mordenite, AlPO-5, A, X, and Y). Free selenium exists in several modifications: a trigonal (t-Se) form containing helical chains,[2] three monoclinic forms (α, β, and γ) containing Se_8 rings,[3-6] a rhombohedral form containing Se_6 rings,[7] and possibly an orthorhombic form containing Se_7 rings.[8] Only the trigonal form is thermodynamically stable at room temperature and pressure. Upon absorption into a molecular sieve matrix, any of these forms (or a combination of these forms) may be adopted. Extended X-ray absorption fine structure (EXAFS),[9] optical absorption, and magic angle spinning solid-state nuclear magnetic resonance (MASNMR) have been used to characterize the selenium-loaded molecular sieves. The study was initiated to try to distinguish differences between the forms taken by selenium in the various sieves and to correlate this with the bulk properties.

Table I

sample	source	chem anal. wt % Al	chem anal. wt % Se	sample treatment time, h/temp, °C
Se-M-9	Grande-Paroise (France)	4.63	8.64	3/150
Se-AlPO5-15	AlPO-5 (Linde)	17.55	15.07	2/150
Se-A-6	zeolite 5A (Linde)	15.97	6.09	8/150
Se-X-26	Linde-13X	9.65	26.20	5/200
Se-Y-34	Linde-LZY-52	5.68	33.84	3/130

To date no three-dimensional analysis of data collected on Se-loaded molecular sieves has been published, although in a study of sodium zeolite A loaded with 23 wt % sulfur, Seff[10] found two equivalent S_8 rings in the crown conformation occupying the large cavity of this molecular sieve. Recently, EXAFS and optical absorbance spectra have been reported for selenium-loaded mordenite.[11] The existence of single chains of Se in the essentially one-dimensional (1D) pore system of this sieve and a shortening of the Se–Se distance by some 2%, as compared to that in crystalline (trigonal) selenium, was reported.

Experimental Section

Sample Nomenclature. The samples are designated according to the scheme Se-MS-WT, where Se = selenium, MS = molecular sieve type, and WT = weight percent of selenium taken up. For example, Se-

* To whom correspondence should be addressed at the Department of Inorganic Chemistry, University of Sydney, Sydney, NSW 2006, Australia.
† Contribution No. 4281.
‡ E. I. du Pont de Nemours and Company.
§ University of New Mexico.
∥ Brookhaven National Laboratory.

(1) Brus, L. E. *J. Phys. Chem.* **1986**, *90*, 2555.
(2) Cherin, P.; Unger, P. *Inorg. Chem.* **1978**, *6*, 1589.
(3) Cherin, P.; Unger, P. *Acta Crystallogr., Sect. B: Struct. Crystallogr. Cryst. Chem.* **1972**, *B28*, 313–317.
(4) Burbank, R. D. *Acta Crystallogr.* **1952**, *5*, 236.
(5) Marsh, R. E.; Pauling, L.; McCullough, J. D. *Acta Crystallogr.* **1953**, *6*, 71.
(6) Foss, O.; Janickis, V. *J. Chem. Soc., Dalton Trans.* **1980**, 624–627.
(7) Miyamoto, Y. *Jpn. J. Appl. Phys.* **1980**, *19*, 1813–1819.
(8) Takahashi, T.; Yagi, S.; Sagawa, T.; Nagata, K.; Miyamoto, Y. *J. Phys. Soc. Jpn.* **1985**, *54*, 1018–1022.
(9) Lee, P. A.; Citrin, P. H.; Eisenberger, P.; Kincaid, B. M. *Rev. Mod. Phys.* **1981**, *53*, 769–803.
(10) Seff, K. *J. Phys. Chem.* **1972**, *18*, 2601–2605.
(11) Tamura, K.; Hosokawa, S.; Endo, H.; Yamasaki, S.; Oyanagi, H. *J. Phys. Soc. Jpn.* **1986**, *55*, 528.

0020-1669/88/1327-0221$01.50/0